

# Black Hole Cross Section at the Large Hadron Collider

Douglas M. Gingrich

*Department of Physics, University of Alberta, Edmonton, AB T6G 2G7 Canada  
 TRIUMF, Vancouver, BC V6T 2A3 Canada  
 gingrich@ualberta.ca*

**Abstract** Black hole production at the Large Hadron Collider (LHC) was first discussed in 1999. Since then, much work has been performed in predicting the black hole cross section. In light of the start up of the LHC, it is now timely to review the state of these calculations. We review the uncertainties in estimating the black hole cross section in higher dimensions. One would like to make this estimate as precise as possible since the predicted values, or lower limits, obtain for the fundamental Planck scale and number of extra dimensions from experiments will depend directly on the accuracy of the cross section. Based on the current knowledge of the cross section, we give a range of lower limits on the fundamental Planck scale that could be obtained at LHC energies.

**Keywords:** black holes, extra dimensions, beyond Standard Model

## 1 Introduction

Models with large[1, 2, 3] or warped[4, 5] extra dimensions allow the fundamental scale of gravity to be as low as the electroweak scale. For energies above the gravity scale, black holes can be produced in particle collisions. This opens up the possibility to produce black holes at the Large Hadron Collider (LHC). The cross section is approximately given by the horizon area of the black hole. Once formed, the black hole can decay by emitting Hawking radiation. The final fate of the black hole is under much debate: quantum gravity will be involved and a stable remnant is possible. If produced at the LHC, black holes will not only allow us to test classical gravity and probe extra dimensions, but will also teach us about quantum gravity.

Over the last seven years there has been much debate over the form of the black hole production cross section in particle collisions. Early discussions postulated a  $\pi R_S^2$  form for the cross section,[6, 7, 8] where  $R_S$  is the Schwarzschild radius of the black hole formed in the hard scattering. This naive form has been criticised[9, 10] and defended[11, 12, 13] over the years. It is well known that this simple form does not take into account the angular momentum of the black hole. Attempts have been made to account for angular momentum in a heuristic way by multiplying the simple expression for the cross section by a form factor.[14, 15, 16, 17] Still, recent work most often takes the form factor to be unity.

Calculations based on classical general relativity have had limited success in improving the cross section estimates.[18, 19] The effects of mass, spin, charge, and finite size of the incoming particles are usually neglected. The effects of finite size have been discussed,[20] and only recently have angular momentum or charge been considered.[21, 22] Although the calculations are far from complete, they do indicate that the simple geometric cross section is correct if multiplied by a formation factor, which has a value at most of about three for seven extra dimensions. These calculations have also been criticised[23] and defended over the years.[24]

Not all of the available energy in a hard parton collision will be trapped behind the event horizon of the black hole. Although it is not known how the energy will be lost, most energy will probably be lost to gravitational radiation into the bulk during the collision. The effects of trapped energy can become important when calculating the particle-level cross section since they result in lowering the mass of the black hole that can be produced for a given hard parton collision. Although only lower limits on the trapped energy have been calculated,[21] these limits allow us to recalculate the particle level cross sections with the assumption of trapped energy. The resulting lower cross sections could modify previous phenomenological results on black hole production at the LHC.

An outline of this paper is as follows. In section 2, we clearly state our assumptions and approximations. This helps define the class of models considered. A review of the classical parton cross section is given in section 3. In section 4, we discuss and write down the particle-level cross section. A variety of improvements to the classical cross section are discussed in section 5. We also summarize cross section results from some other models. In section 6, estimates of the form factor are given. We take trapped energy into account and give limits on the cross section in section 7. And finally in section 8, we derive lower limits on the Planck scale based on the best estimates of the cross section. Black hole decays are not discussed in this paper.

## 2 Assumptions and Approximations

Black hole solutions in higher dimensions have a complicated dependence on both the gravitational field of the brane and the geometry of the extra dimensions. Test particles of a sufficiently high energy to resolve a distance as small as the Planck length are predicted to gravitationally curve, and thereby to significantly disturb, the very spacetime structure that they are meant to probe. However, there are two useful approximations that may be used for a wide class of solutions.[7]

1. The brane is expected to have a tension given by roughly the Planck or string scale. Moreover, the brane on which the Standard Model particles live, will have a gravitational field that should be accounted for in solving Einstein's equations.[25, 26] For black holes with mass  $M$  substantially heavier than the fundamental Planck scale in higher dimensions  $M_D$ ,  $M \gg M_D$ , the brane's field should be negligible and the production process for black holes should be non-perturbative. We will assume that the only effect of the brane field is to bind the black hole to the brane, and that otherwise

the black hole may be treated as an isolated object in the extra dimensions. This is often referred to as the “probe brane approximation”. The effects of quantum gravity will be small under this approximation.

2. If the geometrical scales of the extra dimensions  $R$  (radii, curvature radii, variation scale of the warp factor) are all large compared to  $1/M_D$ , then there is a wide regime in which the geometry of the extra dimensions plays no essential role. An alternative view of this condition is to only consider black holes with horizon radius  $r_h$  much smaller than the size of the extra dimensions,  $1/M_D < r_h \ll R$ , since the Compton wavelength of a black hole is smaller than its horizon radius for most of the parameter space. For large flat dimensions, the topology of the black hole can be assumed to be spherically symmetric in  $(n + 3)$ -spatial dimensions, and the boundary conditions from the compactification can be neglected.

Within this region of applicability, it is often a good approximation to consider the high-energy collision of the particles and the black hole formed to be in  $(n + 4)$ -dimensional flat spacetime. The above two conditions will be used to define the class of models under which we will examine the black hole cross section. In addition, we assume the lifetime of the black hole is long enough so that it behaves as a well-defined quasi-stable state. Some alternative forms of the cross section have been derived under different conditions and will be briefly mentioned.

### 3 Classical Parton Cross Section

The black hole is defined as any matter or energy trapped behind the horizon formed by the available mass and energy of the particle collision. For a particular amount of available energy, a range of black hole masses will result depending on the impact parameter of the particle collision. For an impact parameter  $b \leq r_h$ , the incident relativistic particles pass within the horizon. Formation of the horizon should occur before the particles come in causal contact and would be a classical process. Once inside the horizon, no matter how strong the subsequent QCD effects become, formation of an excited black hole state results. The production of a black hole in high energy collisions would be a totally inelastic process.

In the high-energy limit, in which the classical picture is valid, a black hole can be formed for any incident center of mass energy. The black hole should not be thought of as a single massive degree of freedom, but rather as an intermediate “resonance” with effectively a continuum of states representing the large number of black hole masses.

Since the black hole is not an ordinary particle of the Standard Model and its correct quantum theoretical treatment is unknown, it is treated as a quasi-stable state, which is produced and decays according to the semiclassical formalism of black hole physics. Using the above approximations, it has been argued that at high energies black hole production has a good classical description.[7, 8] This leads to the naive estimate that the cross section for black hole production is approximately given by the classical geometric cross section

$$\hat{\sigma} = \pi R_S^2, \quad (1)$$

where  $R_S$  is the  $(n+4)$ -dimensional Schwarzschild radius corresponding to the black hole mass  $M$  (see appendix for the explicit form of the horizon radius). It depends on the fundamental Planck scale  $M_D$  and the number of extra dimensions  $n$ . In the high-energy limit, the cross section should depend on the impact parameter  $b$ , and a range of black hole masses will result for a given center of mass energy. Since the cross section is dominated geometrically by large impact parameters  $b \gtrsim R_S$ , the average black hole mass should be of the order of the center of mass energy,  $\langle M \rangle \lesssim \sqrt{\hat{s}}$ . In Eq. (1), it is assumed that the black hole mass is given by  $M = \sqrt{\hat{s}}$ . The expression does not contain any small coupling constants that we have to compare to perturbative physics processes; the black hole cross section grows much faster than any known perturbative local physics. The expression for the cross section only contains the fundamental Planck scale as a coupling constant.

In calculating the parton-level cross section and comparing with previous work, it is important to be aware of the many different conventions for the Planck scale. In addition, there are different conventions for the extra-dimensional Newton constant and the definition of the compactification radius  $R$ . Throughout this paper we used the Particle Data Group (PDG)[27] definition of the Planck scale

$$M_D^{n+2} = \frac{1}{8\pi G_N} \frac{1}{R^n}, \quad (2)$$

where  $G_N$  is Newton's constant in four dimensions. This convention is often referred to as the Giudice, Rattazzi, Wells[28] or GRW convention. Another very popular convention that leads to a simple form for the cross section is given by Dimopoulos and Landsberg[8] (DL convention)

$$M_{\text{DL}}^{n+2} = \frac{1}{G_N} \frac{1}{(2\pi R)^n}. \quad (3)$$

Although differences in the conventions can be ignored for astrophysical or cosmological work, they are important and must be taken into account at LHC energies. The DL convention has a weaker dependence on  $n$  than the PDG convention. For  $M_D = M_{\text{DL}}$ , the cross section given by the PDG convention is greater than that of the DL convention for  $n \geq 2$  (see appendix)[30]. To illustrate the effect the definition of the Planck scale can have, we plot the parton cross section versus black hole mass in Fig. 1(a) and 1(b) using the PDG and DL conventions for the Planck scale, respectively. We plot dimensionless quantities for the cross section and mass to emphasize the differences due to the Planck scale conventions. The effect of the Planck scale definition on the dimensionless cross section is significant for most black hole masses and number of extra dimensions.

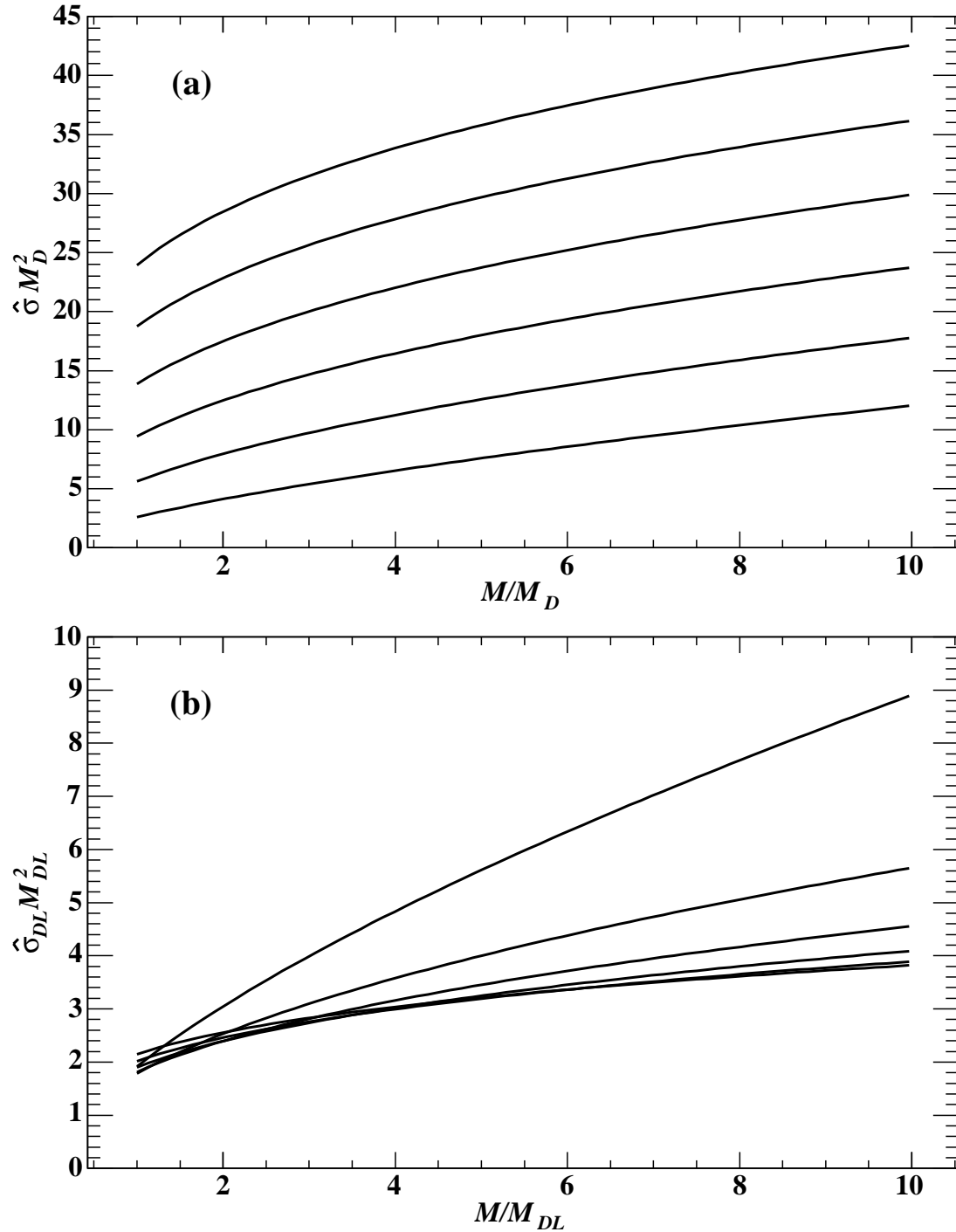


Figure 1: Parton cross section (units of inverse Planck scale squared) versus black hole mass (units of Planck scale) for different  $n$ . (a) PDG definition of Planck scale;  $\hat{\sigma} M_D^2$  increases as  $n = 2-7$ . (b) Dimopoulos and Landsberg definition of Planck scale;  $\hat{\sigma}_{DL} M_{DL}^2$  decreases as  $n = 2-7$ .

## 4 Particle Cross Section

Only a fraction of the total center of mass energy  $\sqrt{s}$  in a proton-proton collision is available in the hard scattering process. We define

$$sx_a x_b \equiv s\tau \equiv \hat{s}, \quad (4)$$

where  $x_a$  and  $x_b$  are the fractional energies of the two partons relative to the proton energies. The full particle-level cross section  $\sigma$  is obtained from the parton-level cross section  $\hat{\sigma}$  by using

$$\sigma_{pp \rightarrow BH+X}(s) = \sum_{a,b} \int_{\frac{M^2}{s}}^1 dx_a \int_{\frac{M^2}{x_a s}}^1 dx_b f_a(x_a) f_b(x_b) \hat{\sigma}_{ab \rightarrow BH}(\hat{s} = M^2), \quad (5)$$

where  $a$  and  $b$  are the parton types in the two protons, and  $f_a$  and  $f_b$  are parton distribution functions (PDFs) for the proton. The sum is over all possible quark and gluon pairings. The parton distributions fall rapidly at high relative energies, and so the particle-level cross section also falls at high energies.

The momentum scale  $Q$  at which the parton distribution functions are evaluated is determined by the inverse length scale associated with the scattering process. For perturbative hard scattering in a local field theory this momentum scale is given by the momentum transfer, which in the  $s$ -channel is the parton-parton center of mass energy:  $Q \sim \sqrt{\hat{s}}$ . For the non-perturbative process of  $s$ -channel black hole formation in a theory of classical gravity, the relevant length scale is the horizon, rather than the black hole mass:  $Q \sim R_S^{-1}$  [31]. This makes sense since the size of the black hole horizon is bigger than its Compton wavelength.

Throughout this paper we use the CTEQ6L1 (leading order with leading order  $\alpha_s$ ) parton distributions functions[32] within the Les Houches Accord PDF framework[33]. We have taken  $Q = R_S^{-1}$  for the scale.

Making a change of variables from  $(x_a, x_b)$  to  $(\tau, x)$  in Eq. (5) gives

$$\sigma_{pp \rightarrow BH+X}(s) = \sum_{a,b} \int_{\frac{M^2}{s}}^1 d\tau \int_{\tau}^1 \frac{dx}{x} f_a\left(\frac{\tau}{x}\right) f_b(x) \hat{\sigma}_{ab \rightarrow BH}(\hat{s} = M^2). \quad (6)$$

The differential cross section can be written as

$$\frac{d\sigma_{pp \rightarrow BH+X}}{d\tau}(s) = \sum_{a,b} \int_{\frac{M^2}{s}}^1 \frac{dx}{x} f_a\left(\frac{\tau}{x}\right) f_b(x) \hat{\sigma}_{ab \rightarrow BH}(\hat{s} = M^2). \quad (7)$$

Since  $\hat{s} = M^2$ , we can make a changing of variable from  $\tau$  to  $M$ ,  $dM/d\tau = s/(2M)$ , to obtain

$$\frac{d\sigma_{pp \rightarrow BH+X}}{dM}(s) = \frac{2M}{s} \sum_{a,b} \int_{M^2/s}^1 \frac{dx}{x} f_a\left(\frac{\tau}{x}\right) f_b(x) \hat{\sigma}_{ab \rightarrow BH}(\hat{s} = M^2). \quad (8)$$

In terms of parton luminosity (or parton flux), we write

$$\frac{d\sigma_{pp \rightarrow BH+X}}{dM} = \frac{dL}{dM} \hat{\sigma}_{ab \rightarrow BH}, \quad (9)$$

where

$$\frac{dL}{dM} = \frac{2M}{s} \sum_{a,b} \int_{M^2/s}^1 \frac{dx}{x} f_a\left(\frac{\tau}{x}\right) f_b(x). \quad (10)$$

The differential cross section thus factorizes for the case of  $\hat{s} = M^2$ . It can be written as the product of the parton cross section time a luminosity function. The parton cross section is independent of the parton types and depends only on the black hole mass, Planck scale, and number of extra dimensions. The parton luminosity function contains all the information about the partons. Beside a dependence on black hole mass, it is independent of the characteristics of the higher-dimensional space, i.e. the Planck scale and number of extra dimensions. The dependence on the black hole mass occurs in the proportionality, the limit of integration, and in the scale of the parton density functions. If the horizon is used as the distance scale in the parton density functions, the luminosity function will depend indirectly on the Planck scale and number of extra dimensions.

For a fixed proton-proton center of mass energy, the parton luminosity function can be pre-calculated to obtain a function depending only on the single mass parameter. Figure 2 shows the parton luminosity function versus black hole mass for  $\sqrt{s} = 14$  TeV for different choices of the QCD scale in the parton density functions for the proton. The choice of scale is clearly significant at high black hole masses. Thus the particle-level cross section does not truly factorize if the horizon radius is used as the QCD scale in the parton density functions for the proton. The steep decrease in Fig. 2 with black hole mass kills any rise in the parton cross section with black hole mass. Nevertheless, if the Planck scale is at the TeV level, particle scattering in the  $s$ -channel will be dominated by black hole production.

The transition from the parton-level to the hadron-level cross section is based on a factorization formula. The validity of this formula for the energy region above the Planck scale is unclear. Even if factorization is valid, the extrapolation of the parton distribution functions into this transplanckian region based on Standard Model evolution from present energies is questionable, since the evolution equations neglect gravity. To proceed, we ignore these difficulties.

## 5 Improvements to the Cross Section

In studying the uncertainties in Eq. (1), it is useful to examine a more general form of the cross section

$$\sigma = F\pi r_h^{2+k} \Theta(M - M_{\min}), \quad (11)$$

where  $F$  is a form factor (usually approximated as unity),  $r_h$  is a more general horizon that may depend on the angular momentum and charges of the black hole (usually taken to be the non-spinning non-charged Schwarzschild radius in  $(n+4)$ -dimensions),  $k$  is the number of extra dimensions in which the Standard Model particles can propagate (usually taken as  $k = 0$ ), and  $\Theta$  is a Heaviside step function that allows black hole production only above some threshold mass  $M_{\min}$  (often implicitly assumed). Implicit in Eq. (11) is the possibility that

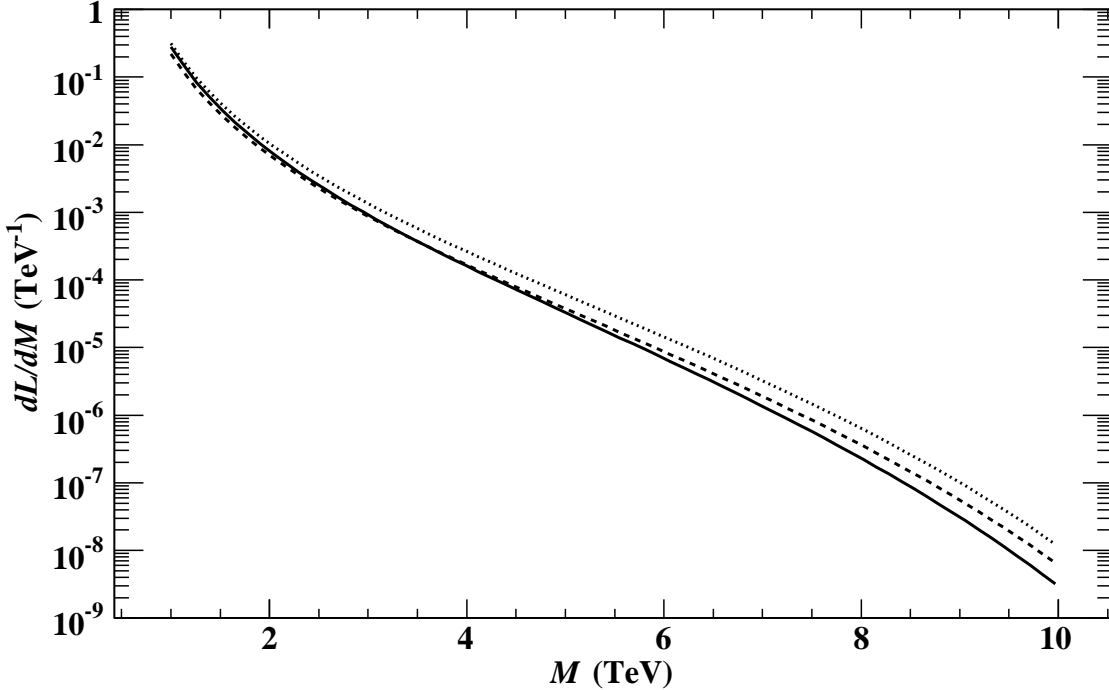


Figure 2: Parton luminosity versus black hole mass. Solid curve  $Q = M$ , dashed curve  $Q = R_S^{-1}$  with  $M_D = 1$  TeV and  $n = 0$ , and dotted curve  $Q = R_S^{-1}$  with  $M_D = 1$  TeV and  $n = 7$ .

each of the factors may depend on the black hole mass, angular momentum, and charges, as well as the fundamental Planck scale and number of extra dimensions. In addition,  $M < \sqrt{s}$  needs to be considered to allow for the possibility of not all the available energy being trapped behind the horizon. We now comment on each of the possible modifications to Eq. (1) in Eq. (11).

### 5.1 Form Factor

Semiclassical considerations give rise to a form factor that reflects the theoretical uncertainties in the dynamics of the process. They take into account that not all of the initial center of mass energy is captured behind the horizon, or account for the distribution of black hole mass as function of energy and angular momentum. In general, the form factor will depend on the parton center of mass energy, the resulting black hole mass, and angular momentum, as well as the fundamental Planck scale and number of extra dimensions. Most studies take the numerical value of the form factor to be unity but we suggest it be accounted for by using the results given below.

## 5.2 Horizon Radius

An intermediate resonance produced in a parton-parton collision must carry the gauge and angular momentum quantum numbers of the initial parton pair. In the high-energy limit, black hole states exist with gauge and angular momentum quantum numbers corresponding to any possible combination of partons within the proton. Thus spinning black holes are expected to be produced at colliders. Although qualitatively equivalent to non-spinning black holes, the results for spinning black holes are expected to be quantitatively quite different and probably more realistic. The Kerr solutions for a spinning black hole in  $(n + 4)$ -dimensional flat spacetime have been calculated[34] (see appendix). The horizon thus depends on the black hole mass and angular momentum, as well as the fundamental Planck scale and number of extra dimensions.

In general, the Kerr solutions should be used for  $r_h$  but a single functional form for all dimensions does not exist. It is usual to make a heuristic argument about the relationship between the angular momentum and horizon radius or maximum impact parameter, and then to obtain an approximate expression for the horizon radius in all dimensions. It is convenient to write this expression as the Schwarzschild radius times an angular momentum-dependent form factor (see appendix).

In the following, we will ignore that the black hole could have charges depending on the partons involved in the hard collision. Such considerations could give rise to the exciting possibility of a naked singularity or a black hole remnant. Much attention has been given to the decay process but very little to the production process of a charged black hole[35]. However, Yoshino and Mann[22] have recently examined head-on collisions of ultra-relativistic charges. They boosted the Reissner-Nordström spacetime to the speed of light. Using the slice at the instant of collision, they studied formation of the apparent horizon and derived a condition indicating that a critical value of the electric charge is necessary for formation to take place. They showed that the presence of charge could decrease the black hole production rate at the LHC. Since this work is very preliminary, we consider the topic of charge to be outside the class of models that we are considering.

Other interesting models, based on assumptions outside of those considered here, have been put forward to obtain distinct forms of the horizon. Rocha and Coimbra-Araújo[26] have recently solved Einstein's equations on the brane to derive the exact form of the brane-world-corrected perturbations in Kerr-Newman metric singularities. Rizzo[36] has performed an analysis in the Randall-Sundrum model with an extended action containing Gauss-Bonnet terms. He obtained expressions for the black hole production cross section in this model. As in the flat scenario, the cross sections are large. A mass threshold below which the black hole will not be produced comes about from a restriction on the Hawking temperature being positive. This gives the cross section a steplike behaviour near  $M_D$ . Rizzo[37] has also examined the modifications to black hole properties due to the existence of spacetime non-commutativity in string theory. In some cases, these models can give significant modifications to the cross section.

### 5.3 Transmission in the Bulk

There are scenarios, such as fat branes or universal extra dimensions[38, 39], in which the Standard Model particles are allowed, to some extent, to propagate in the space dimensions other than the normal  $(3 + 1)$ -dimensions. If gauge bosons are allowed to propagate in the extra dimensional spacetime, their interactions would be modified beyond any acceptable phenomenological limits unless the size of the extra dimensions are very small. Such models can give rise to string balls and  $p$ -branes, as well as black holes. The cross section for producing black holes will be modified and can be substantial larger than that given in Eq. (1).[40, 41, 42] In scenarios in which the Standard Model particles also propagate in the extra dimensions, the incoming partons must collide with an impact parameter in the extra dimensions, which is less than  $r_h$  in all dimensions in order to produce a black hole. Therefore, the cross section for producing a black hole must scale as  $r_h^{2+k}$ , where  $k$  is the number of extra dimensions in which the Standard Model particles propagate, not necessarily equal to  $n$  the total number of extra dimensions.

The power of 2 in Eq. (1) is the result of considering the Standard Model particles to propagate on a 3-brane. In almost all studies of black hole production at colliders this assumption is made. We will thus consider this assumption to define our model and will put  $k = 0$  in Eq. (11). However, we point out that models allowing for non-vanishing  $k$  could give similar signatures to black hole production and thus result in the nonsensical experimental determination of the fundamental Planck scale and the number of extra dimensions if ignored.

Another interesting result arises from split fermions models. In split fermion models, most problems with TeV-scale gravity can be solved if different fermions are localized at different points in the extra dimensions.[43, 44] Dai, Starkman, and Stojkovic[45] have examined black holes and their angular momentum distribution in models with split fermions. They find that the total production cross section is reduced compared with models where all the fermions are localized at the same point in the extra dimensions.

### 5.4 Mass Threshold

There exists a threshold for black hole production. In classical general relativity, two point-like particles in a head-on collision with zero impact parameter will always form a black hole, no matter how large or small their energy. At small energies, we expect this to be impossible due to the smearing of the wave function by the uncertainty relation. This then results in a necessary minimal energy to allow the required close approach. The threshold is of order  $M_D$ , though the exact value is unknown since quantum gravity effects should play an important role for the wave function of the colliding particles. Such a threshold arises naturally in certain types of higher order curvature gravity.[46] For simplicity, it is usual to set this threshold equal to  $M_D$ .

In the high-energy limit, if the impact parameter is less than  $r_h$ , a black hole with mass  $M \sim \sqrt{s}$  can be produced. To avoid quantum gravity effects and stay in the classical regime, we require  $M \geq M_{\min}$ , where  $M_{\min}$  should be a few times larger than  $M_D$ , although it is often taken as  $M_D$ . A reasonable criterion for  $M_{\min}$  is given by the requirement of large

entropy.[47] In the following, we will find it useful to define the dimensionless parameter

$$x_{\min} = \frac{M_{\min}}{M_D}, \quad (12)$$

and require  $x_{\min} \gg 1$ . Unfortunately, all the results will now depend on the subjective choice of the  $x_{\min}$  cutoff.

## 5.5 Trapped Energy

Classical general relativistic calculations indicate that the mass of a black hole formed in a head-on collision is somewhat less than the total center of mass energy; the scattering is not completely inelastic. This is because gravitational radiation is expected to dominate, and because the energy-momentum multipole moments generated during the process of formation have values within the Standard Model brane.[7] Thus Eq. (1) should be modified by replacing the black hole mass by a fraction of the available center of mass energy, leading to a reduction in the cross section. Suggestions for how to treat trapped energy are given below.

## 5.6 Exponential Suppression and Quantum Gravity

Models introducing an exponential suppression of the classical cross section have been formulated. Voloshin[9, 10] suggested an exponential suppression of the geometric cross section based on a Gibbons-Hawking[48] action argument. Detailed subsequent studies performed in simple string theory models, using full general relativistic calculations or a path integral approach, do not confirm this finding, and prove that the geometric cross section is modified only by a numerical factor of order one, at least up to energies of about  $10M_D$ . Solodukhin[11] applied a consistent treatment of both the path integral and statistical approaches suggested in Ref. [9], and found no such exponential suppression. A flaw in the Gibbons-Hawking action argument was further found. The use of this action implies that the black hole has already formed, so describing the evolution of the two colliding particles before they cross the horizon and form the black hole.[12] The most direct undoing of Voloshin's argument has been made by Rychkov[13], which resulting in an erratum by Voloshin[29]. It has further been shown by Rizzo[30] that the black hole cross section, even with the Voloshin suppression factor, can be large. We consider the debate to be resolved, and will not consider a Voloshin exponential suppression factor.

Even if a full description of quantum gravity is not yet available, there are some general features reappearing in most candidates for such a theory: the need for higher dimensions and the existence of a minimal length scale. String theory, as well as non-commutative quantum mechanics, suggest that the Planck length acts as a minimal length in nature, providing a natural ultraviolet cutoff and a limit to the possible resolution of spacetime. The minimal-length effects thus become important in the same energy range in which the black holes are expected to form.

The influence of minimal-length scale on the production of black holes in a model with large extra dimensions was examined by Hossenfelder.[46] The finite resolution of spacetime,

which is caused by the minimal length, results in an exponential suppression of black hole production. At LHC energies, the total cross section is about a factor of five smaller under this scenario. While this is an interesting scenario, we will not address aspects of quantum gravity in this paper.

## 6 Estimates of the Form Factor

Based on the above comments, we now take the black hole cross section to be given by

$$\hat{\sigma} = F\pi R_S^2 \Theta(x_{\min} - 1). \quad (13)$$

In the following, we show that the Kerr solution along with heuristic angular momentum arguments lead to an  $n$  dependent form factor times the Schwarzschild radius, and that general relativistic calculations likewise lead to similar results.

### 6.1 Heuristic Angular Momentum Arguments

Due to the conservation of angular momentum, the angular momentum  $J$  of the formed black hole only vanishes completely for central collisions with zero impact parameter. In the general case for impact parameter  $b$ , there will be an angular momentum  $J = 2(b/2)(\sqrt{\hat{s}}/2) = b\sqrt{\hat{s}}/2$ . The black hole will typically be formed with large angular momentum components. Since the impact parameter is only non-vanishing in directions along the brane, the angular momentum lies within the brane directions. The direction of the angular momentum axis within the Standard Model brane is perpendicular to the collision axis in the high-energy limit.

One may improve estimates of the cross section by taking into account the angular momentum dependence of the horizon radius. Park and Song[14] made an early attempt to incorporate angular momentum into the cross section. They assumed that the semiclassical reasoning for the non-rotating black hole was still valid for rotating black holes. They replaced the Schwarzschild radius by the Kerr solution, and said the total cross section is the sum of the individual spin cross sections up to the maximum possible spin  $MR_S$ :

$$\hat{\sigma} = \sum_{J=0}^{MR_S} \hat{\sigma}(J) = \sum_{a=0}^{\frac{1+n}{2}} \left( \frac{1}{1+a^2} \right)^{\frac{2}{1+n}} \hat{\sigma}(J=0), \quad (14)$$

where  $a = (2+n)J/(2MR_S)$ . The individual spin cross sections  $\hat{\sigma}(J > 0)$  are smaller than the non-spin cross section, and they decrease with increasing spin; this behaviour is counter intuitive. However, the total cross section obtained by summing the rotating and non-rotating cross sections is about 2 to 3 times higher than the non-rotating case.

Kotwal and Hays[15] have analyzed the angular momentum distribution of black holes by computing the production probability using the partial wave expansion of the initial state. They assumed a step-function interaction Hamiltonian with an arbitrary normalization. Two choices for the phase space were examined: purely geometric (no phase space) and number of available states given by the entropy. Fairly different results were obtained depending

on the phase space used. No overall normalization was provided and nor was a closed-form expression obtained for the cross section. We find this model of little practical use for making predictions at the LHC.

One expects the maximum impact parameter will occur near a value of  $b$  that equals the corresponding angular momentum dependent radius  $r_h$ . Using the radius of a Kerr black hole and substituting  $J = r_h M/2$ , Anchordoqui *et al.*[16] obtained

$$F(n) = \left[ 1 + \frac{(n+2)^2}{16} \right]^{\frac{-2}{n+1}}. \quad (15)$$

This result give  $F = 0.63$  to  $0.64$  for  $n = 0$  to  $7$ . This correction is approximately a constant of order unity.

An improved heuristic argument has been given by Ida, Oda, and Park.[17] A black hole is formed when

$$b \leq 2r_h(\sqrt{\hat{s}}, J) = 2r_h(M, bM/2). \quad (16)$$

Since the right hand side is a monotonically decreasing function of  $b$ , there is a maximum value  $b_{\max}$  that saturates the inequality. When  $b = b_{\max}$ , the rotation parameter takes the maximal value, and one obtains

$$F(n) = 4 \left[ 1 + \left( \frac{n+2}{2} \right)^2 \right]^{\frac{-2}{n+1}}. \quad (17)$$

The results using this form factor are given in the row labeled  $F_{\text{IOR}}$  in Table 1. This correction increases the cross section at most by 1.9 for  $n = 7$ .

Since the element of impact parameter  $[b, b + db]$  contributes to the cross section an amount  $2\pi b db$ , the relationship between  $b$  and  $J$  gives us the differential cross section of a black hole with element of angular momentum  $[J, J + dJ]$ :

$$\frac{d\hat{\sigma}}{dJ} = \frac{8\pi J}{\hat{s}} \Theta(J_{\max} - J), \quad (18)$$

where  $J_{\max} = MR_S$ . The differential cross section linearly increases with angular momentum. We expect that this behaviour is correct as a first approximation, so that black holes tend to be produced with large angular momentum. Integrating Eq. (18) gives Eq. (17) times the classical cross section.

We point out that these heuristic angular-momentum arguments only consider the angular momentum of the initial partons; they neglect the spin of the partons.

## 6.2 General Relativistic Analytical Solutions

To improve the naive picture of colliding point particles, we need to consider the grazing collision of particles in  $(n+4)$ -dimensional Einstein gravity and investigate the formation of apparent horizons. A common approach is to treat the creation of the horizon as a collision of two shock fronts in Aichelburg-Sexl geometry.[49] The Aichelburg-Sexl metric is obtained by

boosting the Schwarzschild metric to form two colliding shock fronts. It is assumed that the shock waves can be boosted to thin fronts, thus neglecting the uncertainty of the quantum particles. This treatment is justified as the particles with energy  $\sqrt{\hat{s}} > M_D$  have a position uncertainty smaller than their horizon. Due to the high velocity of the moving particles, space time before and after the shocks is almost flat and the geometry can be examined for the occurrence of trapped surfaces,[50, 51, 52, 53] which depend on the impact parameter.

Eardley and Giddings[18] developed a method for finding the apparent horizons for this system. For a nonzero impact parameter, they were only able to solve the problem analytically for the  $n = 0$  case. They obtained a lower limit of  $F(n = 0) > 0.65$ . This result agrees well with the results obtained by Anchordoqui *et al.*[16] based on the heuristic spin arguments above.

Eardley and Giddings also obtain limits on the final mass of the black hole formed in  $n = 0$ . They found a range from  $M > 0.71\sqrt{\hat{s}}$  for  $b = 0$  to  $M > 0.45\sqrt{\hat{s}}$  for  $b = b_{\max}$ . This can be compared with a perturbative analysis that gave  $M \approx 0.8\sqrt{\hat{s}}$ .[51, 52, 53] For higher dimensions, they only solved the  $b = 0$  case to obtain lower bounds on the final black hole mass of  $M > 0.71\sqrt{\hat{s}}$  to  $0.589\sqrt{\hat{s}}$  for  $n = 0$  to 7.

Unfortunately the Eardley and Giddings results are not general enough to be useful for nonzero impact parameters and higher dimensions. The results do suggest the form factors are of order unity and the semiclassical cross section is valid. They also indicate that a significant amount of the initial energy may not be trapped behind the horizon. For more general results, we now turn to the numerical solutions.

### 6.3 General Relativistic Numerical Solutions

Understanding the case of a nonzero impact parameter in higher dimensions is crucial to improving the cross section estimates. The analytic techniques used to study head-on collisions in general relativity are not applicable to collisions at nonzero impact parameter. Thus the claim that a black hole will be produced when  $b < r_h$  can only be expected to be true up to a numerical factor.

Yoshino and Nambu[19] solved this problem numerically for  $n > 0$  and obtained the maximal impact parameter  $b_{\max}$ . They found that the formation of an apparent horizon occurs when the distance between the colliding particles is less than 1.5 times the effective gravitational radius of each particle. Form factors were obtained and are shown as the row labeled  $F_{YN}$  in Table 1. The estimated numerical errors in  $F_{YN}$  are less than 0.4% for all values of  $n$ . The analytical results of Ida, Oda, and Park ( $F_{IOP}$ ) match the numerical results by Yoshino and Nambu ( $F_{YN}$ ), within an accuracy of less than 1.5% for  $n \geq 2$  and 6.5% for  $n = 1$ .

In their analysis, the apparent horizon was constructed on the union of the two incoming shocks: “old slice”. However, this slice is not at all optimal in the sense that there exists other slices located in the future of the old slice. Yoshino and Rychkov[21] improved the analysis by using the optimal slice. They have updated the calculation and find a 40% to 70% increases in the higher-dimensional cross sections. They have also presented rigorous lower bounds on the final irreducible mass of the black hole, and contours of black hole

angular momentum versus mass. The ultimate goal would be to derive a differential cross section depending on mass and angular momentum of the black hole produced for a given  $\sqrt{\hat{s}}$ . The resulting form factors are shown as the row labeled  $F_{\text{YR}}$  in Table 1.

The validity of the setup of the high-energy two-particle system described above has been questioned because of large-curvature effects in the collision of shock waves.[23, 54] However, Giddings and Rychkov[24] have shown that the objections were an artifact of the unphysical classical point-particle limit, and that for a particle described by a small quantum wave packet, large curvatures do not arise.

$n$	0	1	2	3	4	5	6	7
$F_{\text{IOP}}$	1.000	1.231	1.368	1.486	1.592	1.690	1.780	1.863
$F_{\text{YN}}$	0.647	1.084	1.341	1.515	1.642	1.741	1.819	1.883
$F_{\text{YR}}$	0.71	1.54	2.15	2.56	2.77	2.95	3.09	3.20

Table 1: Form factor  $F$  versus the numbers of extra dimensions  $n$  for different calculations.  $F_{\text{IOP}}$  is from reference [17],  $F_{\text{YN}}$  from reference [19] and  $F_{\text{YR}}$  from reference [21].

## 7 Cross Section at the LHC

From the above discussion, we recommend three corrections to the classical cross section:

1. using form factors,
2. allowing for non-trapped energy, and
3. applying a minimum black hole mass cutoff.

For the form factors, we recommend using Eq. (13) with the values of  $F_{\text{YR}}$  given in Table 1. Although these form factors disagree with the other results in Table 1, they are based on the most detailed calculation to date. It would appear that form factors increase the cross section by a factor of a few for large  $n$ , but are irrelevant for order-of-magnitude estimates. The following describes one approach to taking estimates of the non-trapped energy into account, and applying a minimum black hole mass cutoff to final results.

### 7.1 Trapped Energy Estimates

Yoshino and Nambu[19] (updated by Yoshino and Rychkov[21]) have provided rigorous lower bounds on the amount of available energy trapped behind the horizon. We use their data to obtain lower bounds on the black hole cross section. Figure 3 shows the minimum fraction of energy going into the production of the black hole versus scaled impact parameter for different numbers of extra dimensions. These are lower limits and do not depend on the fundamental Planck scale.

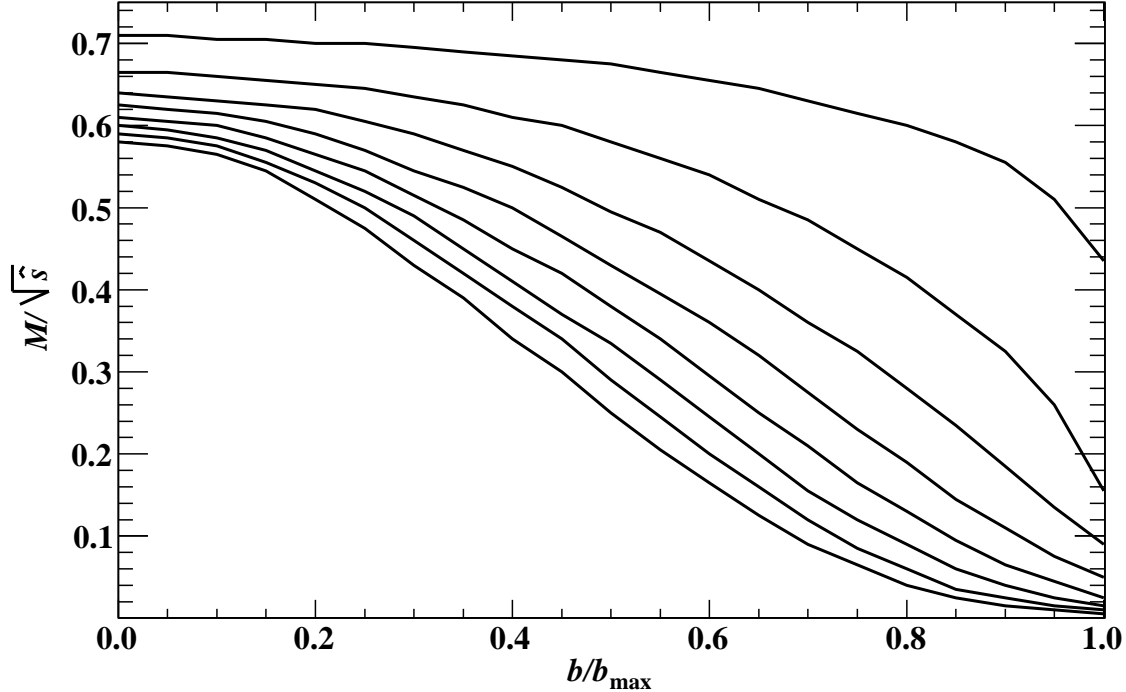


Figure 3: Fractional trapped energy versus scaled impact parameter for different  $n$ . Top curve  $n = 0$  and bottom curve  $n = 7$ . Data taken from Ref. [21].

We see that the lower bound on the black hole mass formed is never more than 71% of the available energy. The fraction of energy available decrease with impact parameter and the number of extra dimensions, from 0.71 to 0.46 for  $n = 0$  to 0.59 to 0 for  $n = 7$ . The mean lower bound on the trapped energies are about 0.6 and 0.27 for  $n = 0$  and 7 respectively. In higher-dimensional spacetime, the amount of “junk” energy increases because the gravitational field distributes in the space of the extra dimensions and only a small portion of the total energy of the system can contribute to the horizon formation. This junk energy will be radiated away rapidly, probably by gravitational radiation in the bulk.

## 7.2 Particle Cross Section

Previous calculations of the cross section for producing a black hole have neglected energy loss in the creation of a black hole, and assumed that the mass of the created black hole was identical to the incoming parton center of mass energy. However, recent work[19, 21] shows the energy loss to gravitational radiation is not negligible, and in fact is large for large number of extra dimensions and for large impact parameters (see Fig. 3).

The trapped mass  $M$  is given by (using the notation of Anchordoqui *et al.*[55])

$$M(z) = y(z)\sqrt{\hat{s}}, \quad (19)$$

where the inelasticity  $y$  is a function of  $z \equiv b/b_{\max}$ . This complicates the parton model calculations, since the production of a black hole of mass  $M$  is lower than  $\sqrt{\hat{s}}$  by  $M/y(z)$ , thus requiring the lower cutoff on the parton momentum fraction to be a function of the impact parameter. We can no longer use the factorized version of the particle-level cross section given by Eqs. (9) and (10).

Following Anchordoqui *et al.*[47, 55], we take the proton-proton cross section as the impact parameter-weighted average over parton cross sections, with the lower parton fractional momentum cutoff determined by the requirement  $M_{\min} = x_{\min} M_D$ . This gives a lower bound  $(x_{\min} M_D)^2/(y^2 s)$  on the parton momentum fraction  $x$ . With this in mind, the  $pp \rightarrow \text{BH} + \text{X}$  cross section becomes

$$\sigma_{pp \rightarrow \text{BH} + \text{X}}(s, x_{\min}) \geq \int_0^1 2zdz \sum_{a,b} \int_{\frac{(x_{\min} M_D)^2}{y^2 s}}^1 d\tau \int_{\tau}^1 \frac{dx}{x} f_a\left(\frac{\tau}{x}\right) f_b(x) \hat{\sigma}_{ab \rightarrow \text{BH}}(\tau s). \quad (20)$$

Since the trapped energy is a lower bound, the resulting cross section is a lower bound.

Taking  $x_{\min} = 1$ , we obtain the families of cross section curves shown in Figs. 4 and 5. The solid curves are for the semiclassical cross section calculated using Eqs. (9), (10), and (13) with the form factors  $F_{\text{YR}}$ . We will henceforth refer to these curves as the semiclassical cross section. The dashed lower curves are given by Eqs. (13) and (20) with the form factors  $F_{\text{YR}}$ . We will henceforth refer to these curves as the trapped surface (TS) cross section. In Figs. 4(a) and 4(b) the different curves of a given type are for different Planck scales, starting from 0.5 TeV for the top curve and decreasing with increasing Planck scale in steps of 0.5 TeV. Figure 4(a) is for  $n = 3$ , while Fig. 4(b) is for  $n = 7$ . In Figs. 5(a) and 5(b) the different curves of a given type are for different numbers of extra dimensions, starting from  $n = 2$  for the top curve and ending at  $n = 7$  for the bottom curve. Figure 5(a) is for a Planck scale of 1 TeV, while Fig. 5(b) is for a Planck scale of 5 TeV.

The effect of non-trapped energy on the cross section is large because the LHC energy is close to the threshold for black hole production and lost energy limits the availability energy for the black hole. The cross section curves show that there is less dependence on  $n$  than  $M_D$ . This is because the  $n$  dependence of the form factor tends to cancel the  $n$  dependence of the horizon radius.[56] It is reasonable to consider the semiclassical cross sections with form factors greater than unity as loose upper bounds on the black hole cross sections, which may increase by a factor of a few as the trapped-surface cross sections increase. We thus take the point of view that the black hole cross section lies between the semiclassical and TS cross sections. The difference can be several orders of magnitude. The TS cross sections cut off at a mass above the trapped energy bounds given by Fig. 3. Applying a cutoff  $x_{\min} > 1$  will further restrict the range of the TS cross sections, as well as the semiclassical cross sections.

## 8 Lower Limits on the Planck Scale

The cross sections in the previous section can be used to predict the discovery limits for a given luminosity, and be used, in principle, to extract the Planck scale and number of extra

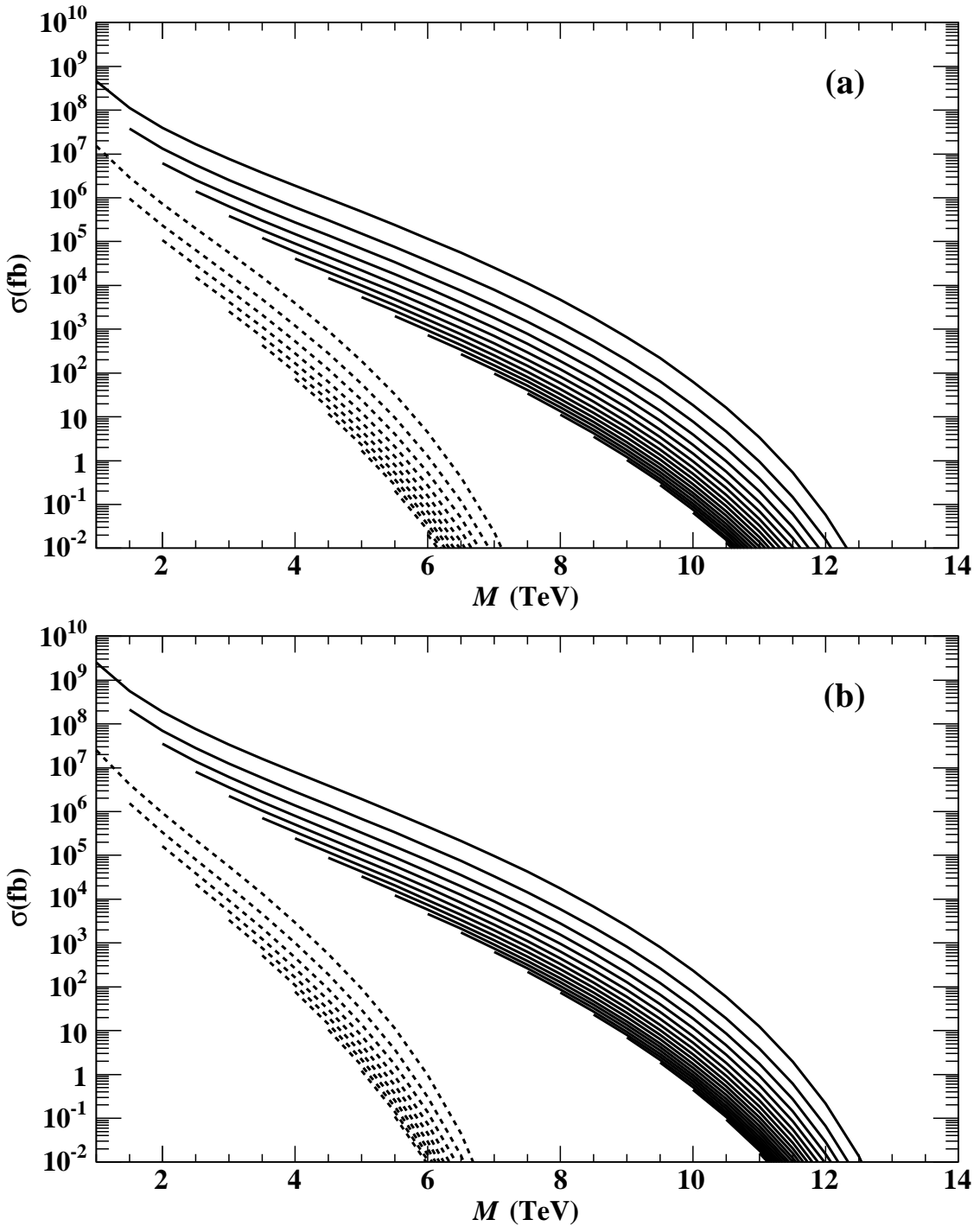


Figure 4: Cross section versus black hole mass. Solid curves semiclassical cross section and dashed curves trapped surface cross section. Curves of same type for different Planck scales, 0.5 TeV top curves decreasing with increasing Planck scale in steps of 0.5 TeV. (a)  $n = 3$  and (b)  $n = 7$ .

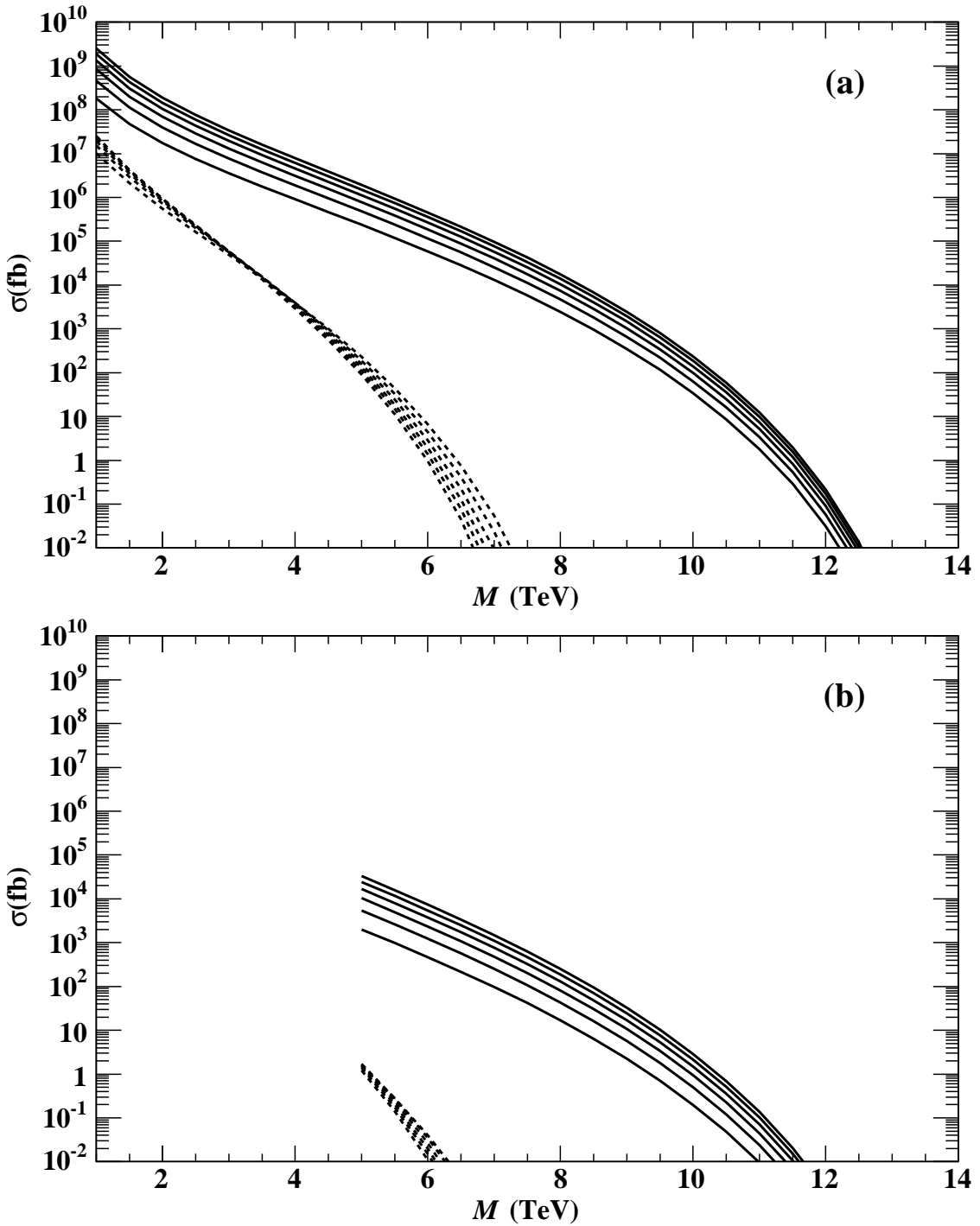


Figure 5: Cross section versus black hole mass. Solid curves semiclassical cross section and dashed curves trapped surface cross section. Curves of same type for different number of extra dimensions, top curves  $n = 2$  and bottom curves  $n = 7$ . (a)  $M_D = 1$  TeV and (b)  $M_D = 5$  TeV.

dimensions. In the event of no detectable black hole signal, the cross sections call also be used to set limits on the Planck scale and number of extra dimensions.

We consider the scenario in which no black hole signal has been observed after the accumulation of an integrated luminosity of  $300 \text{ fb}^{-1}$  at  $\sqrt{s} = 14 \text{ TeV}$ . Rather than study the different decay phases of the black hole and estimate the detector's capabilities for measuring them, we assume a perfect detector. This will give the most optimistic limits possible. Assuming a perfect experiment, the 95% confidence-level upper limit on the cross section is  $10^{-2} \text{ fb}$ . Using this value of the cross section, we have extracted lower limits on the Planck scale  $M_D$  as a function of cutoff parameter  $x_{\min}$  for different values of the number of extra dimensions  $n$ . The results are shown in Fig. 6 for  $n = 2$  to  $7$ . The solid curves were obtained from the semiclassical cross sections. The dashed curves were obtained from the trapped surface cross section bounds. The dotted curves are a result of the mass cutoff in the trapped surface cross sections. The dotted curves can be consider as the infinite luminosity case of the trapped surface predictions. The small spread in the different curves of a given type is due to the different number of extra dimensions.

We can use Fig. 6 to get a feel for how the different cross section models affect the range of Planck-scale limits. For  $x_{\min} = 5$ , a lower limit of  $M_D > 2.4 \text{ TeV}$  is obtained for the semiclassical case and  $M_D > 1.4 \text{ TeV}$  for the TS case. The TS limit can be improved to  $M_D > 1.7 \text{ TeV}$  with infinite luminosity. Relaxing the cutoff criteria used to avoid quantum gravity effects to  $x_{\min} = 3$  gives a lower limit of  $M_D > 3.8 \text{ TeV}$  for the semiclassical case and  $M_D > 2.2 \text{ TeV}$  for the TS case. The TS limit can be improved to  $M_D > 2.8 \text{ TeV}$  with infinite luminosity. There appears to be very little sensitivity to the limits on the Planck scale due to the number of extra dimensions: less than a 3% effect.

## 9 Discussion

The large difference in cross section between the models does not translate into a large difference in the limits on  $M_D$  because both cross sections fall rapidly at low values of the cross section. The limits on  $M_D$  presented here are compatible with the discovery limits that have been determined in previous work.[28, 47, 55, 57, 58, 59] Our limits might appear different due to the stringent requirements on  $x_{\min}$  and the different definition of  $M_D$ . If one is willing to relax the requirement on  $x_{\min}$  and risk entering the quantum-gravity regime, than the differences between the two models becomes significant. This difference presumably still holds when the uncertainties in the black hole decay and experimental effects are taken into account.

It is not possible to compare our results for the limits on  $M_D$  with existing experimental limits. This would require estimating the uncertainties in the black hole decay as well as including the experimental effects. In any case, there are probably methods at the LHC that are more sensitive to setting limits on  $M_D$  than the direct search for black holes.

After seven years, the validity of the naive geometric approximation for black hole cross section still stands. The best modifications we can make at this time is to include the form factor in the last row of Table 1, which ranges from about 2 to 3 when the number of extra

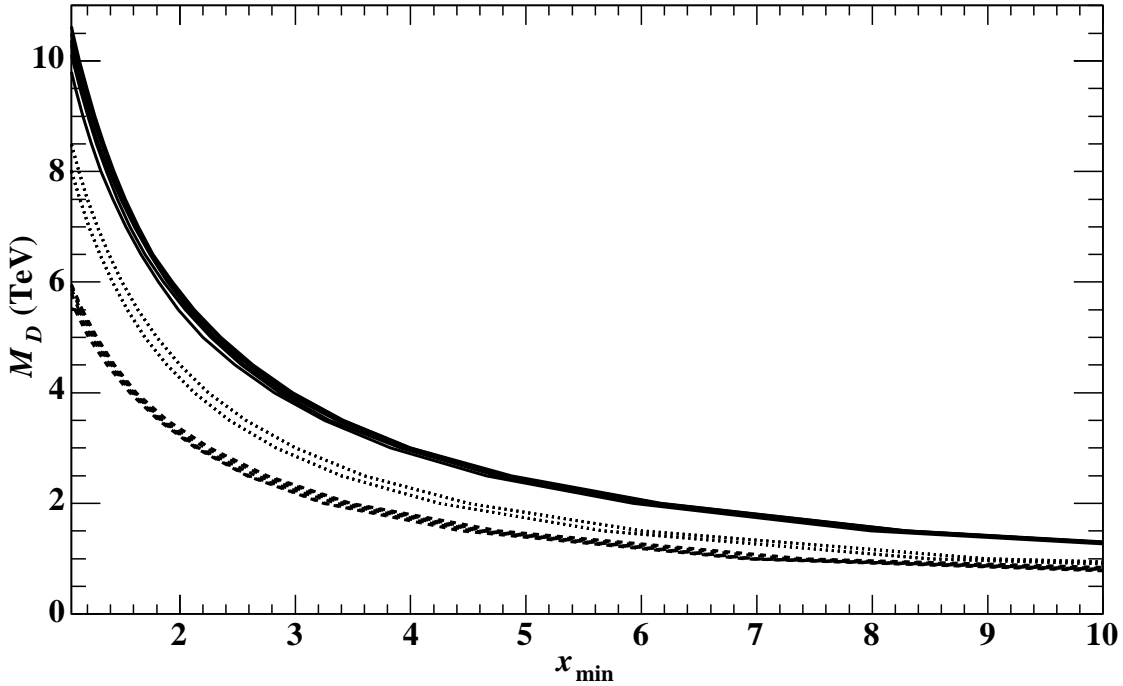


Figure 6: Lower limits on Planck scale as function of cutoff parameter. Solid curves semi-classical case. Dashed curves trapped surface case. Dotted curves result of mass cutoff in trapped surface case. Spread in curves of same type due to different  $n$ .

dimensions ranges from 2 to 7; not a very significant modification when considering the other uncertainties. However, classical general relativity has shown that not all the available energy is trapped behind the horizon and lost energy should be accounted for. Unfortunately, the state of the calculations only allow us to approximate the effects of non-trapped energy.

Ignoring the effects of non-trapped energy on the black hole cross section could have a large affect on TeV-scale gravity studies. This might modify the results of previous phenomenological studies, which are sensitive to the black hole cross section relative to the QCD cross section (see for example Ref. [60, 61]).

The trapped-energy approach only gives a lower bound on the final mass of the black hole. In order to clarify the final mass, different methods such as the direct study of gravitational wave emission are necessary.[54] The problem is extremely difficult because of the nonlinearity of Einstein's equations, and because the high-energy collision of the two particles producing a black hole requires inclusion of nonlinear effects. Cardoso *et al.*[62, 63, 64] have studied gravitational radiation in linear perturbation theory of higher-dimensional flat spacetime. The results are in agreement with the four dimensional estimate of D'Eath and Payne.[51, 52, 53] However, the total energy decreases with the number of extra dimensions, in disagreement with the estimate of Eardley and Giddings.[18]

Recently studies of gravitational radiation in the head-on collision of two black holes in

higher-dimensional spacetime have been made using a close-slow approximation.[65, 66] This system can be regarded as a first simplification of particle collisions. The results agree with the fully nonlinear analysis for four dimensions.

These perturbative approaches probably have an error of a factor of two or more. Since these studies are in the exploratory stage and have not yet been performed as a function of impact parameter in higher dimensions, they are currently of limited usefulness for making predictions at the LHC.

There are many uncertainties in our understanding of black hole production in higher dimensional TeV-scale gravity. Reliable predictions of the cross section are not yet available. We have examined the existing models to explore the different options for filling in the gaps in our understanding. In this way, we hope to be better prepared to confront the possibility of black hole production at the LHC.

*Note added.* While this work was being finished, we learned that some aspects of the topics addressed in this paper were also under consideration by another group; that work has recently appeared in Ref. [67, 68].

## Acknowledgments

This work was supported in part by the Natural Sciences and Engineering Research Council of Canada.

## A *D*-Dimensional Black Hole Horizon Radius

Black hole Kerr solutions to Einstein's equations have been obtained in asymptotically flat higher dimensional spacetime.[34] For distances much smaller than size of the extra dimensions, the event horizon radius for a *D*-dimensional spinning black hole is given by

$$r_h^{D-5} \left[ r_h^2 + \frac{(D-2)^2 J^2}{4M^2} \right] = \frac{16\pi G_D M}{(D-2)\Omega_{D-2}}, \quad (21)$$

where  $J$  is the four-dimensional angular momentum,  $M$  is the mass of the black hole, and  $\Omega_{D-2}$  is the area of a unit  $(D-2)$ -sphere, given by

$$\Omega_{D-2} = \frac{2\pi^{(D-1)/2}}{\Gamma\left(\frac{D-1}{2}\right)}. \quad (22)$$

A common way of writing the horizon radius is

$$r_h = \left[ \frac{1}{1+a^2} \right]^{\frac{1}{D-3}} R_S, \quad (23)$$

where

$$a = \frac{(D-2)J}{2Mr_h} \quad (24)$$

is a rotation parameter depending on the horizon radius, and

$$R_S = \left[ G_D M \left( 2^3 \pi^{(3-D)/2} \frac{\Gamma\left(\frac{D-1}{2}\right)}{(D-2)} \right) \right]^{\frac{1}{D-3}} \quad (25)$$

is the spinless (Schwarzschild) horizon radius. When  $J \rightarrow 0$ ,  $r_h \rightarrow R_S$ .

To express the  $D$ -dimensional Newton constant in terms of the Planck scale, we must choose a convention. Using the PDG convention (our convention)

$$M_D^{D-2} = \frac{(2\pi)^{D-4}}{8\pi G_D} = \frac{(2\pi)^n}{8\pi G_D}, \quad (26)$$

the horizon radius is

$$\begin{aligned} R_S &= \frac{1}{M_D} \left[ \frac{M}{M_D} \left( 2^{D-4} \pi^{(D-7)/2} \frac{\Gamma\left(\frac{D-1}{2}\right)}{D-2} \right) \right]^{\frac{1}{D-3}} \\ &= \frac{1}{M_D} \left[ \frac{M}{M_D} \left( 2^n \sqrt{\pi}^{(n-3)} \frac{\Gamma\left(\frac{n+3}{2}\right)}{n+2} \right) \right]^{\frac{1}{n+1}}. \end{aligned} \quad (27)$$

(28)

Using the convention of Dimopoulos and Landsberg[8]

$$M_{\text{DL}}^{D-2} = \frac{1}{G_D}, \quad (29)$$

the horizon radius is

$$R_S = \frac{1}{\sqrt{\pi} M_{\text{DL}}} \left[ \frac{M}{M_{\text{DL}}} \left( \frac{8\Gamma\left(\frac{D-1}{2}\right)}{D-2} \right) \right]^{\frac{1}{D-3}} \quad (30)$$

$$= \frac{1}{M_{\text{DL}}} \left[ \frac{M}{M_{\text{DL}}} \left( 2^3 \sqrt{\pi}^{(-n-1)} \frac{\Gamma\left(\frac{n+3}{2}\right)}{n+2} \right) \right]^{\frac{1}{n+1}}. \quad (31)$$

Although the Dimopoulos and Landsberg convention results in a simpler expression for the Planck scale Eq. (29) and the cross section Eq. (30), experimental limits are most often set on the Planck scale in the PDG convention Eq. (26).

Setting the black hole mass equal in the two conventions for the horizon radii Eq. (28) and Eq. (31), the ratio of the cross sections can be written as[30]

$$\frac{\hat{\sigma}}{\hat{\sigma}_{\text{DL}}} = \left[ \frac{(2\pi)^n}{8\pi} \right]^{\frac{2}{n+1}} \left[ \frac{M_{\text{DL}}^2}{M_D^2} \right]^{\frac{n+2}{n+1}}. \quad (32)$$

For  $M_{\text{DL}} = M_D$ , the ratio of the cross sections is 1.4 for  $n = 2$  and 11.1 for  $n = 7$ .

## References

- [1] N. Arkani-Hamed, S. Dimopoulos and G. Dvali, “The hierarchy problem and new dimensions at a millimeter,” *Phys. Lett.* **B429**, 263 (1998); arXiv:hep-ph/9803315.
- [2] I. Antoniadis, N. Arkani-Hamed, S. Dimopoulos and G. Dvali, “New dimensions at a millimeter to a fermi and superstrings at a TeV,” *Phys. Lett.* **B436**, 257 (1998); arXiv:hep-ph/9804398.
- [3] N. Arkani-Hamed, S. Dimopoulos and G. Dvali, “Phenomenology, astrophysics, and cosmology of theories with submillimeter dimensions and TeV scale quantum gravity,” *Phys. Rev.* **D59**, 086004 (1999); arXiv:hep-ph/9807344.
- [4] L. Randall and R. Sundrum, “Large Mass Hierarchy from a Small Extra Dimension,” *Phys. Rev. Lett.* **83**, 3370 (1999); arXiv:hep-ph/9905221.
- [5] L. Randall and R. Sundrum, “An Alternative to Compactification,” *Phys. Rev. Lett.* **83**, 4690 (1999); arXiv:hep-th/9906064.
- [6] T. Banks and W. Fischler, A Model for High Energy Scattering in Quantum Gravity, arXiv:hep-th/9906038.
- [7] S. B. Giddings and S. Thomas, “High energy colliders as black hole factories: The end of short distance physics,” *Phys. Rev.* **D65**, 056010 (2002); arXiv:hep-ph/0106219.
- [8] S. Dimopoulos and G. Landsberg, “Black Holes at the Large Hadron Collider,” *Phys. Rev. Lett.* **87**, 161602 (2001); arXiv:hep-ph/0106295.
- [9] M. B. Voloshin, “Semiclassical suppression of black hole production in particle collisions,” *Phys. Lett.* **B518**, 137 (2001); arXiv:hep-ph/0107119.
- [10] M. B. Voloshin, “More remarks on suppression of large black hole production in particle collisions,” *Phys. Lett.* **B524**, 376 (2001); arXiv:hep-ph/0111099.
- [11] S. N. Solodukhin, “Classical and quantum cross-section for black hole production in particle collisions”, *Phys. Lett.* **B533**, 153 (2002); arXiv:hep-ph/0201248.
- [12] A. Jevicki and J. Thaler, “Dynamics of black hole formation in an exactly solvable model,” *Phys. Rev.* **D66**, 024041 (2002); arXiv:hep-th/0203172.
- [13] V. S. Rychkov, “Topics in Black Hole Production,” Cargèse Summer School, June 7-19, 2004, 363-369; arXiv:th/0410295.
- [14] S. C. Park and H. S. Song, “Production of Spinning Black Holes at colliders,” *J. Korean Phys. Soc.* **43**, 33 (2003); arXiv:hep-ph/0111069.

- [15] A. V. Kotwal and C. Hays, “Production and decay of spinning black holes at colliders and tests of black hole dynamics,” *Phys. Rev.* **D66**, 116005 (2002); arXiv:hep-ph/0206055.
- [16] L. Anchordoqui, J. L. Feng, H. Goldberg and A. D. Shapere, “Black holes from cosmic rays: Probes of extra dimensions and new limits on TeV-scale gravity,” *Phys. Rev.* **D65**, 124027 (2002); arXiv:hep-ph/0112247.
- [17] D. Ida, K. ya Oda and S. C. Park, “Rotating black holes at future colliders: Greybody factors for brane fields,” *Phys. Rev.* **D67**, 064025 (2003); Erratum-ibd. **D69**, 049901 (2004); arXiv:hep-th/0212108.
- [18] D. M. Eardley and S. B. Giddings, “Classical black hole production in high-energy collisions,” *Phys. Rev.* **D66**, 044011 (2002); arXiv:gr-qc/0201034.
- [19] H. Yoshino and Y. Nambu, “Black hole formation in the grazing collision of high-energy particles,” *Phys. Rev.* **D67**, 024009 (2003); arXiv:gr-qc/0209003.
- [20] E. Kohlprath and G. Veneziano, “Black holes from high-energy beam-beam collisions,” *J. High Energy Phys.* **0206**, 057 (2002); arXiv:gr-qc/0203093.
- [21] H. Yoshino and V. S. Rychkov, “Improved analysis of black hole formation in high-energy particle collisions,” *Phys. Rev.* **D71**, 104028 (2005); arXiv:hep-th/0503171.
- [22] H. Yoshino and R. B. Mann, “Black hole formation in the head-on collision of ultarelativistic charges,” *Phys. Rev.* **D74**, 044003 (2006); arXiv:gr-qc/0605131.
- [23] V. S. Rychkov, “Black hole production in particle collisions and higher curvature gravity,” *Phys. Rev.* **D70**, 044003 (2004); arXiv:hep-ph/041116.
- [24] S. B. Giddings and V. S. Rychkov, “Black holes from colliding wavepackets,” *Phys. Rev.* **D70**, 104026 (2004); arXiv:hep-th/0409131.
- [25] A. N. Aliev and A. E. Gümrükçüoğlu, “Charged rotating black holes on a 3-brane”, *Phys. Rev.* **D71**, 104027 (2005); arXiv:hep-ph/0607027.
- [26] R. Rocha and C. H. Coimbra-Araújo, “Extra dimensions in LHC via mini-black holes: effective Kerr-Newman brane-world effects”, *Phys. Rev.* **D74**, 055006 (2006); arXiv:hep-ph/0607027.
- [27] Particle Data Group (W.-M. Yoa *et al.*), *J. Phys. G* **33**, 1165 (2006).
- [28] G. F. Giudice, R. Rattazzi and J. D. Wells, “Transplanckian Collisions at the LHC and Beyond,” *Nucl. Phys.* **B630**, 293 (2002); arXiv:hep-ph/0112161.
- [29] M. B. Voloshin, Erratum to: “More remarks on suppression of large black hole production in particle collisions” [Phys. Lett. B 524 (2002) 376], *Phys. Lett.* **B605**, 426 (2005).

- [30] T. G. Rizzo, “Black Hole Production Rates at the LHC: Still Large,” eConf C010630, P339 (2001); arXiv:hep-ph/0111230.
- [31] R. Emparan, M. Masip and R. Rattazzi, “Cosmic rays as probes of large extra dimensions and TeV gravity,” *Phys. Rev.* **D65**, 064023 (2002); arXiv:hep-ph/0109287.
- [32] J. Pumplin, D. R. Stump, J. Huston, H. L. Lai, P. Nadolsky and W. K. Tung, “New Generation of Parton Distributions with Uncertainties from Global QCD Analysis,” *J. High Energy Phys.* **0407**, 012 (2002); arXiv:hep-ph/0201195.
- [33] LHAPDF the Les Houches Accord PDF Interface, Version 5.2.2, maintained by M. Whalley; <http://hepforge.cedar.ac.uk/lhapdf/>.
- [34] R. C. Myers and M. J. Perry, “Black Holes in Higher Dimensional Space-Times,” *Ann. Phys. (N.Y.)* **172**, 304 (1986).
- [35] B. Koch, M. Bleicher and S. Hossenfelder, “Black hole remnants at the LHC,” *J. High Energy Phys.* **0510**, 053 (2005); arXiv:hep-ph/0507138.
- [36] T. G. Rizzo, TeV-Scale Black Holes in Warped Higher-Curvature Gravity, arXiv:hep-ph/0510420.
- [37] T. G. Rizzo, Noncommutative Inspired Black Holes in Extra Dimensions, *J. High Energy Phys.* **0609**, 021 (2006); arXiv:hep-ph/0606051.
- [38] S. Dimopoulos and R. Emparan, “String balls at the LHC and beyond,” *Phys. Lett.* **B526**, 393 (2002); arXiv:hep-ph/0108060.
- [39] R. Casadio and B. Harms, “Can black holes and naked singularities be detected in accelerators?,” *Int. J. Mod. Phys.* **A17**, 4635 (2002); arXiv:hep-th/0110255.
- [40] E.-J. Ahn, M. Cavaglià and A. V. Olinto, “Brane factories”, *Phys. Lett.* **B551**, 1 (2003); arXiv:hep-th/0201042.
- [41] K. Cheung and C.-H. Chou, “ $p$ -brane production in Fat brane or Universal extra dimensions scenario,” *Phys. Rev.* **D66**, 036008 (2002); arXiv:hep-ph/0205284.
- [42] K. Cheung, “Black hole, string ball, and  $p$ -brane production at hadronic supercolliders,” *Phys. Rev.* **D66**, 036007 (2002); arXiv:hep-ph/0205033.
- [43] N. Arkani-Hamed and M. Schmaltz, “Hierarchies without Symmetries from Extra Dimensions,” *Phys. Rev.* **D61**, 033005 (2000); arXiv:hep-ph/9903417.
- [44] N. Arkani-Hamed, Y. Grossman and M Schmaltz, “Split Fermions in Extra Dimensions and Exponentially Small Cross-Sections at Future Colliders,” *Phys. Rev.* **D61**, 115004 (2000); arXiv:hep-ph/9909411.

[45] D.-C. Dai, G. D. Starkman and D. Stojkovic, “Production of black holes and their angular momentum distribution in models with split fermions,” *Phys. Rev.* **D73**, 104037 (2006); arXiv:hep-ph/0605085.

[46] S. Hossenfelder, “Suppressed black hole production from minimal length,” *Phys. Lett.* **B598**, 92 (2004); arXiv:hep-ph/0404232.

[47] L. Anchordoqui, J. L. Feng, H. Goldberg and A. D. Shapere, “Inelastic black hole production and large extra dimensions,” *Phys. Lett.* **B594**, 363 (2004); arXiv:hep-ph/0311365.

[48] G. W. Gibbons and S. W. Hawking, “Action integrals and partition functions in quantum gravity,” *Phys. Rev.* **D15**, 2752 (1977).

[49] P. C. Aichelburg and R. U. Sexl, “On the Gravitational Field of a Massless Particle,” *Gen. Rel. Grav.* **2**, 303 (1971).

[50] R. Penrose (unpublished, reported in Ref. [53])

[51] P. D. D’Eath and P. N. Payne, “Gravitational radiation in black-hole collisions at the speed of light. I. Perturbation treatment of the axisymmetric collision,” *Phys. Rev.* **D46**, 658 (1992).

[52] P. D. D’Eath and P. N. Payne, “Gravitational radiation in black-hole collisions at the speed of light. II. Reduction to two independent variables and calculation of the second-order news function,” *Phys. Rev.* **D46**, 675 (1992).

[53] P. D. D’Eath and P. N. Payne, “Gravitational radiation in black-hole collisions at the speed of light. III. Results and conclusions,” *Phys. Rev.* **D46**, 694 (1992).

[54] V. Cardoso, E. Berti and M. Cavaglià, “What we (don’t) know about black hole formation in high-energy collisions,” *Class. Quant. Grav.* **22**, L61 (2005); arXiv:hep-ph/0505125.

[55] L. Anchordoqui, J. L. Feng, H. Goldberg and A. D. Shapere, “Updated limits on TeV-scale gravity from the absence of neutrino cosmic ray showers mediated by black holes,” *Phys. Rev.* **D68**, 104025 (2003); arXiv:hep-ph/0307228.

[56] B. Webber, “Black Holes at Accelerators,” eConf C0507252, T030 (2005); arXiv:hep-ph/0511128.

[57] E.-J. Ahn M. Cavaglià and A. V. Olinto, “Uncertainties in limits on TeV-gravity from neutrino-induced showers,” *Astropart. Phys.* **22**, 377 (2005); arXiv:hep-ph/0312249.

[58] J. Tanaka, T. Yamamura, S. Asai and J. Kanzaki, “Study of black holes with the ATLAS detector at the LHC,” *Eur. Phys. J.* **C41**, s02 19 (2005); arXiv:hep-ph/0411095.

- [59] C. M. Harris, M. J. Palmer, M. A. Parker, P. Richardson, A. Sabetfakhri and B. R. Webber, “Exploring higher dimensional black holes at the Large Hadron Collider,” *J. High Energy Phys.* **0505**, 053 (2005); arXiv:hep-ph/0411022.
- [60] L. Lönnblad, M. Sjödahl and T. Åesson, “QCD-suppression by Black Hole Production at the LHC,” *J. High Energy Phys.* **0509**, 019 (2005); arXiv:hep-ph/0505181.
- [61] L. Lönnblad and M. Sjödahl, “Classical and Non-Classical ADD-phenomenology with high- $E_\perp$  jet observables at collider experiments,” *J. High Energy Phys.* **0610**, 088 (2006); arXiv:hep-ph/0608210.
- [62] V. Cardoso, O. J. C. Dias and P. S. Lemos, “Gravitational radiation in  $D$ -dimensional spacetimes,” *Phys. Rev.* **D67**, 064016 (2003); arXiv:hep-th/0212168.
- [63] V. Cardoso, P. S. Lemos and S. Yoshida, “Electromagnetic radiation from collisions at almost the speed of light: An extremely relativistic charged particle falling into a Schwarzschild black hole,” *Phys. Rev.* **D68**, 084011 (2003); arXiv:gr-qc/0307104.
- [64] E. Berti, M. Cavaglià and L. Gualtieri, “Gravitational energy loss in high energy particle collisions: Ultrarelativistic plunge into a multidimensional black hole,” *Phys. Rev.* **D69**, 124011 (2004); arXiv:hep-th/0309203.
- [65] H. Yoshino, T. Shiromizu and M. Shibata, “Close-limit analysis for head-on collision of two black holes in higher dimensions: Brill-Lindquist initial data,” *Phys. Rev.* **D72**, 084010 (2005); arXiv:gr-qc/0508063.
- [66] H. Yoshino, T. Shiromizu and M. Shibata, “Close-slow analysis for head-on collision of two black holes in higher dimensions: Bowen-York initial data,” *Phys. Rev.* **D74**, 124022 (2006); arXiv:gr-qc/0610110.
- [67] M. Cavaglià, R. Godang, L. Cremaldi and D. Summers, Catfish: A Monte Carlo simulator for black holes at the LHC, arXiv:hep-ph/0609001.
- [68] E.-J. Ahn and M. Cavaglià, “Simulations of black hole air showers in cosmic ray detectors”, *Phys. Rev.* **D73**, 042002 (2006); arXiv:hep-ph/0511159.